

PETROLOGY AND URANIUM DISTRIBUTION IN THE YOUNGER GRANITES OF GABAL ABU DIAB AREA, EASTERN DESERT, EGYPT

MEDHAT M. EL-MANSI

NUCLEAR MATERIALS AUTHORITY, P.O. BOX – 530 MAADI, CAIRO, EGYPT

(Received: 15 June 2005)

ABSTRACT

The area of Gabal Abu Diab (about 92.5 km^2) is located between latitudes 25o 11` and 25o 16` N and longitudes 34o 11` and 34o 17` E. The younger granites of G. Abu Diab are classified on petrographic and geochemical bases as monzogranites, syenogranites and alkali-feldspar granites. They originated from peraluminous, calc-alkaline magma. This magma was derived from crustal sialic materials during post-orogenic magmatism. The field observations, the petrographic characteristics and the geochemical features may suggest that the studied younger granites intruded in successive pulses started with monzogranites and ended with alkali-feldspar granites.

The enrichment of uranium in the alkali-feldspar granites is related to magmatic processes, except minor locations, which suffered secondary processes and limited redistribution of uranium. These secondary processes have leached uranium from the country rocks and even the monzogranites and syenogranites themselves and added it within the microfractures of the alkali-feldspar granites.

INTRODUCTION

The area of Gabal Abu Diab (about 92.5 km^2) is located between latitudes 25° 11` and 25° 16` N and longitudes 34° 11` and 34° 17` E (Fig. 1). The area is characterized by rugged topography due to the presence of moderate to high mountains. G. Abu Diab (1161 m above sea level) represents the highest elevation point in the area. The southern part of the area can be reached using Idfu–Mersa Alam asphaltic road (160 km from Mersa Alam and 63 km from Idfu) and turning northward for about 22 km in a well leveled dusty track.

G.Abu Diab forms a belt extending in the NW-SE direction, and is made of pink granites associated with minor reddish varieties (Amin *et al.*, 1954). Using the Rb-Sr method, the age of Abu Diab pink granites ranges between 533 Ma (Hashad *et al.*, 1972) and 522 Ma (El-Manharawy, 1977). G. Abu Diab younger granites are belonging to the higher differentiated group (lower K/Rb ratios), which is characterized by sodic plagioclase and small amounts or absence of biotite (Sayyah *et al.*, 1973). Abd El-Maksoud (1974) concluded that Abu Diab granites were intruded during consequent pulses of magmatic activity, depending on the morphological and statistical studies of zircons.

ISSN 1012 – 5965

Dardier (1997) classified, petrographically, the younger granites of Gabal Abu Diab into biotite granites, perthitic leucogranites and muscovite granites.

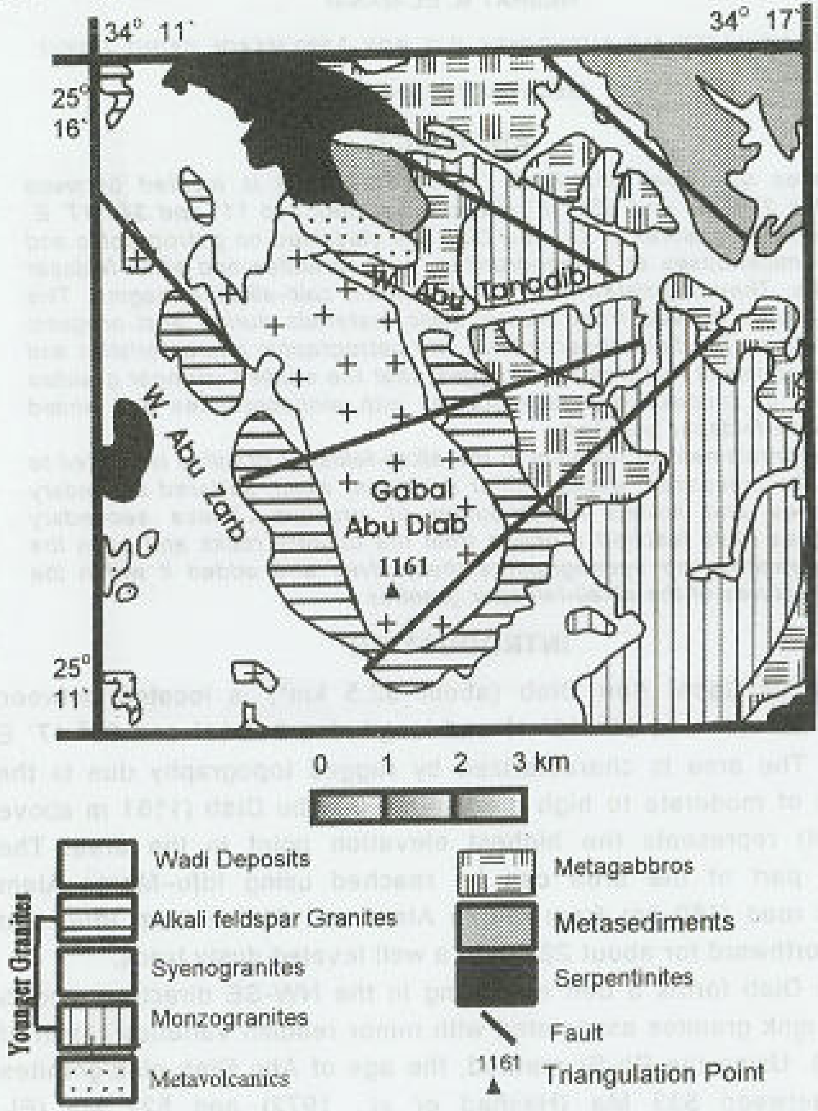

Fig. 1: Geologic map of Gabal Abu Diab Area, Eastern Desert, Egypt (modified after Dardier, 1997)

The main aims of this work could be summarized as following:

1) Detailed petrographic studies,
2) Deducing the magma type and tectonic setting of the studied younger granites, and
3) Studying the factors controlling the distribution of uranium.

GEOLOGIC OUTLINES

G. Abu Diab is mainly surrounded by sandy plains. It is flanked on the northeastern corner and eastern side by the metagabbros and metasediments, while on the northwestern and western sides the serpentinites and metavolcanics exist. Beyond the southern limit of the mapped area, Gabal Abu Diab is intruding the grey granitoids. The contacts between the younger granites and the country rocks are very sharp and usually dip towards the country rocks. Gabal Abu Diab younger granites (especially the eastern loop) take xenoliths of different sizes and shapes from the surrounding country rocks.

G. Abu Diab is formed of eastern and western loops forming an oval-shaped pluton elongated in a NNW - SSE direction. The studied younger granites are medium- to coarse-grained, equigranular or rarely porphyritic, massive, unfoliated rocks. Abu Diab younger granites could be further subdivided into two separate units. The first unit (eastern loop) is greyish pink, with characteristic slight foliation. The second unit (western loop) is common and is of pink-red colour. The granites of the first unit are dissected by larger number of mafic and felsic dykes in contrast to those of the first unit. Moreover, the pink-red granites are highly dissected by quartz and feldspar veinlets, especially along the northwestern peripheries of the pluton. The pink-red granites intrude the greyish pink varieties and sometimes carry them as roof pendants. Three major sets of joints, in decreasing order of abundance, striking E-W, NW-SE and WNW-ESE and dipping 85° to N, 10° to SW and 75° to NE respectively are recognized traversing G. Abu Diab granites.

Generally, the granites of G. Abu Diab are characterized by exfoliation and cavernous weathering with characteristic bouldery appearance and monumental shapes. Alteration is mainly represented by hematization, which renders the granites brick-red colour. On the other hand, silicification and feldspar metasomatism render the granites white colour. Other minor alteration features as epidotization, chloritization, and kaolinization are restricted to fault planes and contacts.

Faults traversing the area are limited in number. They are of variable length (0.2 - 7 km) with vertical or steep dips. Two main perpendicular trends have been recognized; they are N40°W-S40°E and N50°E-S50°W. Dykes invading the mapped lithologic units are numerous and are of variable length and thickness. They whether felsic or mafic, are rectilinear with parallel walls and occur in swarms of strike varying between NNE-SSW and NW-SE with vertical or steep dips (60°-90°) to the NW and NE. The felsic ones are of more resistance to weathering than the enclosing rocks and usually give rise to spines and ridges

PETROGRAPHY

Thirty-four thin sections, representing different varieties of the studied younger granites, were chosen for petrographic studies. The younger granites, in the studied area, could be classified into the following rock types:

A. Monzogranites,
B. Syenogranites, and
C. Alkali-feldspar granites.

A. Monzogranites

Monzogranites are composed of perthites (about 35.39 %), quartz (about 26.15 %), plagioclase (about 28.48 %) and biotite (about 8.19 %) as essential minerals. Apatite, titanite and opaques are accessory minerals (about 1.79 %), while chlorite, kaolinite and muscovite are secondary minerals.

Perthites occur as subhedral to anhedral crystals ranging in size from about 0.28 mm to 2.56 mm across. They are generally of patchy and flame-like types (Fig. 2). Microcline perthite is rarely observed. Perthites are slightly kaolinized and sericitized. Few perthite crystals are corroded by quartz and fresh plagioclase crystals, especially along their peripheries and cleavage planes.

Quartz is found as anhedral crystals of various sizes, ranging from 0.2 to 2.85 mm across. Quartz can be differentiated into two forms. The first and the most abundant form is coarse containing fine inclusions of clay minerals and iron oxides, especially along peripheries and are characterized by irregular or sutured boundaries. This indicates that there was earlier quartz, which was overgrown during a process of silicification. They sometimes show undulose extinction and cracking (Fig. 3) due to local deformation. The second form is undeformed, fine-grained, which may represent a second crystallization stage. Generally, quartz increases in volume with increasing grade of alteration.

Plagioclase presents in variable modal proportions, but is generally less abundant than perthites. The presence of two feldspar phases, perthites and sodic plagioclase, suggests that these granites are mostly subsolvus and crystallized under high water pressure (Greenberg, 1981). Plagioclase occurs as anhedral to subhedral tabular crystals ranging in size from about 0.25 mm to 2.75 mm across. Some plagioclase crystals are engulfed poikilitically in biotite and perthite, while others corrode perthite and other plagioclase crystals, indicating more than one plagioclase generation. This could be proved by the cracking and glide twinning (Fig. 4) of some older plagioclase crystals, while others show clear simple and lamellar twinning. Most plagioclase crystals show selective alteration, where their cores are usually more altered than the outer rims (Fig. 5).

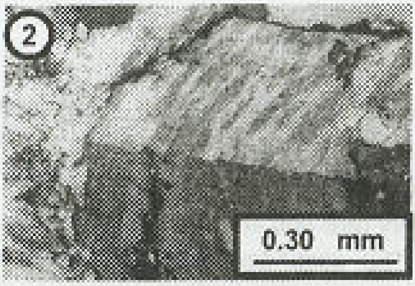

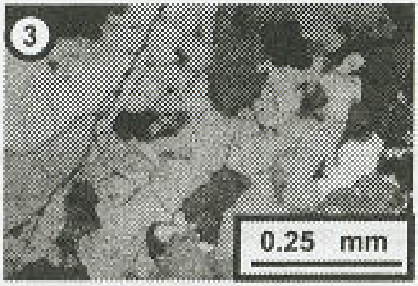

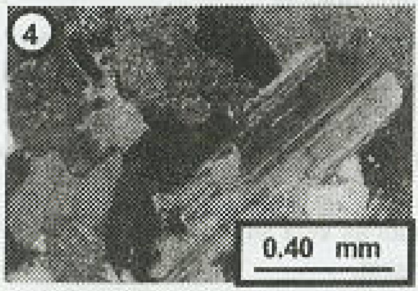

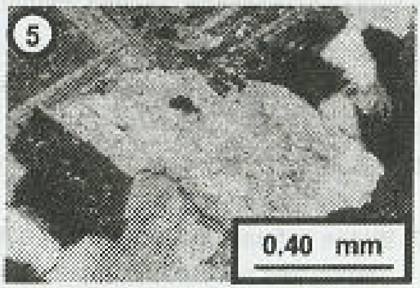

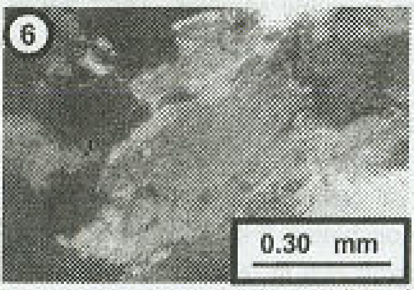

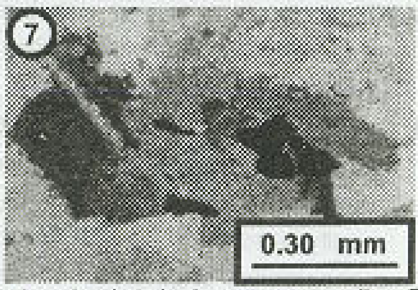

Fig.2: Flame-type orthoclase perthite showing simple twinning, monzogranites, C.N.
Fig.3: Highly cracked quartz showing undulose extinction, monzogranites, C.N.
Fig.4: Plagioclase showing glide twinning, monzogranites, C.N.
Fig.5: Plagioclase with slightly altered cores, monzogranites, C.N.
Fig.6: Slightly altered biotite flake, monzogranites, C.N.
Fig.7: Highly altered (chloritized) biotite, monzogranites, P.L.

Biotite occurs as medium, slightly curved to highly kinked, irregular flakes. The biotite flakes are slightly (Fig. 6) or completely (Fig.7) altered to chlorite, especially along peripheries and cleavage planes. At higher grades of alteration, muscovite is formed. The alteration is accompanied by releasing of iron oxides along peripheries and cleavage planes.

Apatite is found as minute euhedral prismatic and needle-like crystals included in quartz and biotite. Titanite is found as small anhedral to subhedral sphenoid and elongated crystals showing high cracks. It corrodes feldspars and biotite and is corroded by quartz. Iron oxides are found as small irregular patches scattered in the rock. Also, they are found as tiny inclusions in mica, titanite, quartz and feldspars.

B. Syenogranites

Syenogranites are equigranular, coarse- to medium-grained, composed of perthites (about 51.58 %), quartz (about 32.51 %), plagioclase (about 13.49 %) and subordinate amount of mica (about 1.27 %) as essential minerals. The accessory minerals (about 1.15 %) are very rare and are mainly represented by iron oxides with few zircon crystals. The secondary minerals are mainly represented by kaolinite, sericite, chlorite and epidote.

Generally, the syenogranites have the same mineral composition and the same texture of the monzogranites, but with some differences that could be summarized as follows:

1. Alkali feldspars are highly exceeding plagioclase. In some samples, plagioclase becomes very rare.
2. Biotite is found in subordinate amount as very small elongated flakes and sometimes becomes completely absent.
3. Phlogopite is observed with biotite in many samples. Their flakes are sometimes stained with reddish brown colouration due to iron oxides smear along cleavage planes.
4. Syenogranites possess more zircon (Fig. 8), fluorite and apatite crystals than monzogranites, suggesting that syenogranites originated from magma richer in Zr, F and P_2O_5. All previously mentioned minerals are usually surrounded by wide pleochroic haloes (Fig. 9), suggesting that the syenogranites originated from magma rich in radio elements (El-Mansi, 1996).
5. Titanite and apatite are very rare or completely absent.
6. Syenogranites, generally, show less deformation, less undulose extinction in quartz, less granulation along crystal margins, less fracturing in

perthites (Figs. 10 and 11) and more conspicuous twinning in plagioclase (Figs. 12 and 13) than the monzogranites. Accordingly, the syenogranites may represent a later phase after the intrusion of monzogranites.

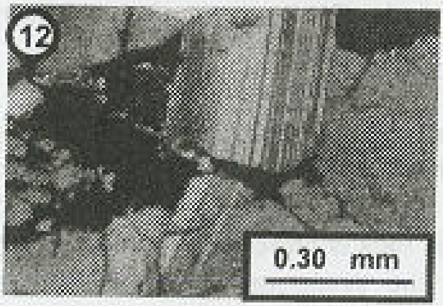

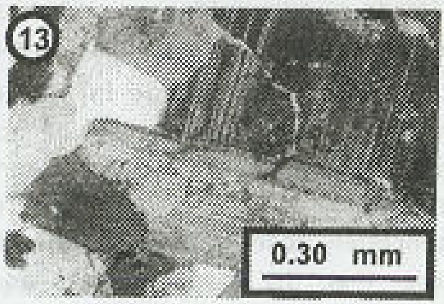

Fig. 8: Quartz enclosing two zircon crystals, which show narrow pleochroic halo, syenogranites, C.N.
Fig. 9: Zircon causing wide pleochroic halo in phlogopite, syenogranites, C.N.
Fig.10: Simply twined flame-type orthoclase perthite, syenogranites, C.N.
Fig.11: Patchy-type orthoclase perthite corroded by quartz, syenogranites, C.N.
Fig.12: Plagioclase showing conspicuous simple and lamellar twinning, syenogranites, C.N.
Fig.13: Plagioclase showing pericline twinning, syenogranites, C.N.

C. Alkali-feldspar granites

Alkali-feldspar granites are generally equigranular, medium- to coarse-grained with hypidiomorphic texture. They are composed of alkali feldspars (about 58.68 %), quartz (about 30.64 %), plagioclase (about 7.2 %) and muscovite (about 2.1 %) with subordinate amount of biotite (about 0.2 %) as essential minerals. The accessory minerals (about 1.18%) are zircon, apatite, lepidolite, fluorite and iron oxides.

Alkali feldspars are represented by orthoclase and microcline perthites as well as non-perthitic microcline. Orthoclase perthite occurs as subhedral to anhedral prismatic crystals ranging in size from 0.3 mm to 2.8 mm across. They are of flame-, string- and patchy-type (Figs. 14 and 15) and sometimes show simple twinning. They usually enclose plagioclase, quartz and micas and are corroded by quartz. Microcline perthite occurs as subhedral crystals ranging in size from 0.2 mm to 2.6 mm across. They corrode plagioclase and orthoclase perthite and include quartz poikilitically. Cracks in perthite facilitate attacking of late iron-rich solutions, which cause iron staining and give the rock its red colouration. These cracks are sometimes empty or filled with iron oxides and/or secondary muscovite. Non-perthitic coarse microcline crystals show conspicuous crosshatched twinning. These crystals corrode quartz, feldspars and muscovite. The presence of microcline crystals may indicate a phase of K-metasomatism.

Quartz crystals range in size from 0.2 mm to 3.1 mm across. It usually contains inclusions of apatite, zircon and muscovite. They corrode plagioclase, mica and perthites (Fig. 16). Also, small quartz crystals are formed as fracture fillings. Undulose extinction is completely absent, indicating that this rock is affected by stresses much lower than the monzogranites and the syenogranites. The cracked quartz crystals are very rare and are restricted to the fault planes; the cracks, if present, are usually filled with iron oxides.

Plagioclase is found as small subhedral to euhedral tabular crystals ranging in size from 0.3 mm to 2.4 mm across. In some samples, plagioclase is a minor phase and occurs mostly as a component of the perthite. The majority of crystals show clear lamellar twinning without visible alteration.

Muscovite is found as irregular medium flakes, corroded by quartz and perthites (Fig. 17). Some muscovite flakes show pleochroic haloes.

It is sometimes encountered as secondary mineral filling cracks or replacing feldspars. In some cases, muscovite flakes appear to be squeezed and deformed due to tectonic stresses or secondary growths of feldspars and quartz crystals. This indicates the primary nature of muscovite. Biotite occurs rarely as small irregular flakes, corroded by quartz, feldspars and fluorite. Lepidolite is found as yellow, elongated, fan-shaped or leaf-like flakes. They occupy the interstitial spaces between the essential minerals and corrode plagioclase, quartz and perthites.

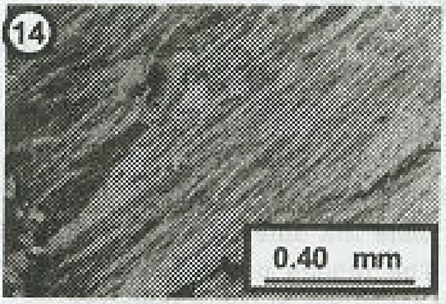

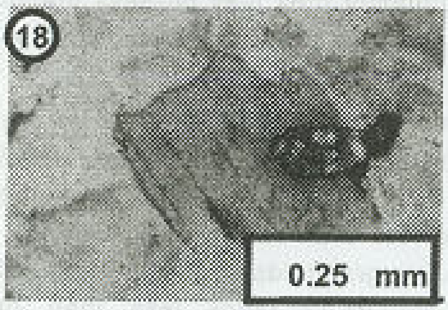

Fig.14: String-type orthoclase perthite, alkali feldspar granites, C.N.
Fig.15: Flame- and patchy type orthoclase perthite, alkali feldspar granites, C.N.
Fig.16: Flame-type orthoclase perthite corroded by quartz, alkali feldspar granites, C.N.
Fig.17: Primary muscovite flake corroded by quartz and feldspar, alkali feldspar granites, C.N.
Fig.18: Metamicted zircon surrounded by wide pleochroic halo, alkali feldspar granites, P.L.
Fig.19: Several needle-like apatite crystals enclosed in quartz, alkali feldspar granites, P.L.

Zircon occurs in a very minor amount as subhedral to euhedral prismatic crystals ranging in size from 0.04 mm to 0.2 mm across. It is found as inclusions in quartz and biotite (Fig. 18). Zircon crystals are usually cloudy and rimmed with iron oxides. Clusters of tiny apatite (Fig. 19) crystals are common in quartz crystals. Fluorite is found as anhedral fine crystals. They are usually colourless with faint green colour. Fluorite is usually associated with iron oxides and/or corroding micas and feldspars.

GEOCHEMISTRY

Twelve samples representing the studied younger granites were selected in order to identify the magma type and tectonic setting. The major elements were determined by wet chemical analysis technique (Shapiro and Brannock, 1962). Thorium was determined spectrophotometrically using Arsenazo III technique. Uranium was analyzed using U-Laser analyzer technique, while the other trace elements were determined using XRF technique. The results of analysis and CIPW-norms as well as some geochemical ratios are given in table (1).

A. Geochemical characteristics

The studied younger granites are characterized by relatively high silica contents (72.09 – 76.31 wt. %) except one sample of monzogranites showing SiO_2 of 70.69 wt. %. The calcium contents decrease gradually from monzogranites to syenogranites and reach the lowest values in the alkali-feldspar granites, which show CaO contents ranging between 0.21 and 0.43 wt. %. Thus, the alkali-feldspar granites are considered as low-calcium granites, and consequently they may possess uranium mineralization (Assaf *et al.*, 1997; Dardier, 1997; Moharem, 1999 and El-Mansi *et al.*, in press).

The three types of younger granites show Fe_2O_3/FeO ratios more than one indicating that these granites have tendency toward the oxidizing conditions (Cox et al. 1979). Moreover, the same authors concluded that Na_2O/K_2O ratios are less than one in the granitoids of crustal origin, but range from 1 to 4.5 in granitoids of mantle origin. The studied younger granites show Na_2O/K_2O ratios less than one suggesting, crustal origin (partial anatexis of pre-existing crustal materials). Only the monzogranites show Na_2O/K_2O greater than one but less than 1.15; this slight excess may be attributed to the contamination with country rocks during crystallization. This conclusion is supported in the field by the presence of numerous xenoliths of the country rocks in the eastern loop (monzogranites of grayish pink colour) of G. Abu Diab

Table (1): Major oxides (wt. %), CIPW-norm and trace elements (ppm) as well as some geochemical parameters for the studied granitic rocks

Rock type	Monzogranites				Syenogranites				Alkali-feldspar granites			
SampleNo.	1	2	3	4	5	6	7	8	9	10	11	12
Symbol	●	●	●	●	○	○	○	○	+	+	+	+
	Major Oxides (wt. %)											
SiO_2	72.09	70.69	72.54	74.27	74.24	74.27	73.38	76.15	74.68	74.06	75.26	75.31
TiO_2	0.93	0.61	0.31	0.12	0.08	0.09	0.06	0.08	0.03	0.04	0.04	0.04
Al_2O_3	13.91	14.64	13.08	13.04	13.1	12.82	13.68	13.63	14.03	14.74	13.51	12.46
Fe_2O_3	1.59	1.34	1.01	1.04	0.92	1.54	1.52	0.43	0.76	0.84	0.31	0.62
FeO	1.13	1.15	0.61	1.3	0.83	0.67	0.84	0.36	0.5	0.45	0.22	0.25
MnO	0.06	0.44	0.07	0.12	0.06	0.11	0.09	0.09	0.03	0.03	0.12	0.06
MgO	0.52	0.73	0.74	0.43	0.47	0.46	0.65	0.15	0.28	0.31	0.16	0.21
CaO	1.36	1.39	1.04	1.12	0.62	0.82	0.76	0.61	0.43	0.21	0.38	0.39
Na_2O	3.02	3.78	3.91	3.18	4.30	3.82	3.86	3.68	4.01	3.74	4.11	4.14
K_2O	3.28	3.33	3.73	3.03	4.56	4.12	4.02	4.01	4.59	4.93	4.99	4.76
P_2O_5	0.62	0.31	0.27	0.36	0.09	0.17	0.15	0.06	0.06	0.06	0.05	0.08
L.O.I.	1.43	1.49	1.50	1.88	0.63	0.80	0.91	0.67	0.56	0.66	0.79	0.61
Total	99.94	99.90	99.62	99.89	99.90	99.09	99.91	99.91	99.96	99.96	99.94	99.93
	CIPW- norm											
Q	40.92	33.0	31.82	42.14	29.77	34.48	33.68	38.30	32.46	32.88	31.42	33.42
Or	19.07	19.87	22.47	18.4	27.19	24.66	24.02	23.91	27.34	29.46	29.8	28.47
Ab	25.82	32.61	33.66	27.42	36.73	32.83	32.87	31.18	34.47	31.63	35.07	35.06
An	3.06	4.99	7.14	3.46	2.57	3.23	2.92	2.76	1.69	0.75	1.61	1.3
C	4.47	3.04	0	3.31	0.13	0.89	1.94	2.25	1.76	2.97	0.76	0
Hy	1.29	2.73	1.84	2.7	1.92	1.19	2.0	0.72	0.92	0.9	0.7	0.8
Mt	1.16	1.94	1.4	1.64	1.33	2.23	2.23	0.63	1.15	1.23	0.45	0.83
He	0.8	0	0.07	0	0	0	0	0	0	0	0	0.07
Il	1.81	1.2	0.66	0.23	0.15	0.17	0.12	0.15	0.06	0.08	0.08	0.08
Ap	1.62	0.73	0.6	0.8	0.2	0.33	0.33	0.11	0.13	0.11	0.11	0.18
D.I.	85.81	86.38	87.95	87.96	93.69	91.87	90.47	93.39	94.27	93.97	96.29	96.95
	Trace elements (ppm)											
Ba	465	690	426	567	389	296	299	296	154	208	163	166
Rb	83	45	81	96	184	155	103	201	236	194	296	299
Sr	134	183	126	160	74	69	89	53	32	53	49	48
Y	23	19	38	26	76	43	88	40	46	53	43	54
Zr	119	74	91	68	168	246	157	223	211	266	186	329
Nb	74	60	80	93	103	115	64	109	105	139	97	119
Th	18	21	23	17	41	36	27	28	118	79	144	105
U	3.8	3.8	4.5	4.1	13.4	11.8	9.1	8.3	91.0	62.5	85.5	72.9
	Geochemical ratios											
Fe_2O_3/FeO	1.4	1.17	1.66	0.8	1.11	2.3	1.81	1.19	1.5	1.87	1.41	2.48
Na_2O/K_2O	0.92	1.14	1.05	1.05	0.94	0.93	0.96	0.92	0.87	0.76	0.82	0.87
Rb/Sr	0.62	0.25	0.64	0.59	2.49	2.25	1.16	3.79	7.38	3.66	6.04	6.23
Zr/Sr	0.89	0.39	0.73	0.42	2.23	3.62	1.74	4.29	6.26	5.02	3.8	7.16
K/Rb	306.8	624.2	386.9	266.4	204.6	223.4	330.2	166.4	162.1	213.9	139.9	133.1
Th/U	4.74	5.53	5.11	4.15	3.06	3.05	2.97	3.37	1.26	1.25	1.68	1.44

The differentiation index (D.I. = Q + Or + Ab; Thronton and Tuttle, 1960) values increase gradually from monzogranites (85.4 – 88) to syenogranites (90.5 - 93.7) and reach the highest values in the case of alkali-feldspar granites (94 - 97). Also, Rb/Sr and Zr/Sr ratios show increasing in the same trend.

Generally, the studied three granitic types can be considered as highly differentiated granites. The granitic rocks derived from upper mantle show K/Rb ratios ranging between 700 and 1500, while the granitic rocks derived from sialic crustal materials show lower ratios (Heier, 1973). In this work, the studied younger granites show K/Rb ratios less than 390 confirming a crustal origin.

B. Geochemical classification, magma type and tectonic setting

On Streckeisen and Le Maitre (1979) diagram, the studied younger granites plot in the monzogranite, syenogranite and alkali-feldspar granite fields (Fig. 20a). The studied younger granites originated from calc-alkaline (Fig. 20b) peraluminous (Fig. 20c) magma. They are considered as S-type granites (Fig. 20d) derived from crustal sialic materials during post-orogenic magmatism (Figs. 20e).

The crustal thickness during the emplacement of the monzogranites ranges between 20 and 30 km, while both syenogranites and alkali-feldspar granites originated in a crust of thickness greater than 30 km (Fig. 20f). It is worth to mention that the alkali-feldspar granites emplaced in a crust of slightly greater thickness than the syenogranites. Starting with monzogranites to syenogranites and finally with the alkali-feldspar granites, the crustal thickness increases gradually, suggesting that the studied younger granites intruded in successive pulses.

DISTRIBUTION OF URANIUM

Alkali-feldspar granites show high uranium contents (62.5 to 91 ppm) relative to those of monzogranites (3.8 to 4.5 ppm) and syenogranites (8.3 to 13.4 ppm). Generally, U, Th, Zr and Rb behave compatibly in granitic melt, so that where uranium concentration is controlled by magmatic processes, these elements would be expected to increase (Briqueu *et al.* 1984; El-Mansi, 1993; Dardier, 1997 and El-Mansi et al., in press). In the studied alkali-feldspar granites, the excess in Zr, Th, D.I., Rb/Sr and Zr/Sr is accompanied by conspicuous excess in uranium (Fig. 21). The results indicate magmatic origin of uranium. In other words, the alkali-feldspar granites originated from magma rich in uranium. Normally, Th is three times as abundant as U in granitic rocks (Rogers and Adams, 1969). When Th/U ratio is disturbed, it indicates addition or removal of uranium because thorium is relatively stable during post magmatic processes.

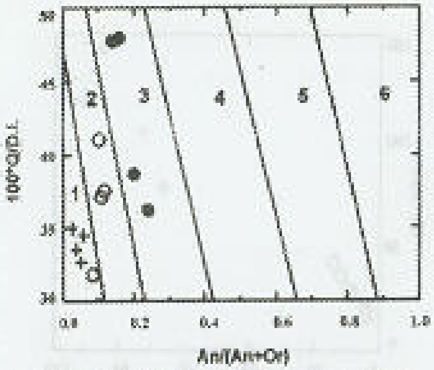

(a) Streckeisen and Le Maitre (1979)

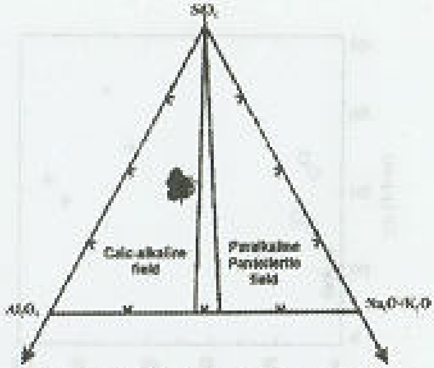

(b) Mac Donald and Bailey (1973)

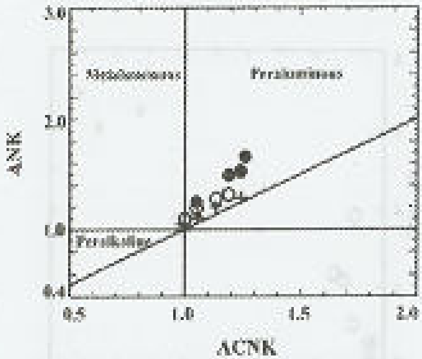

(C) Maniar and Picolli (1989)

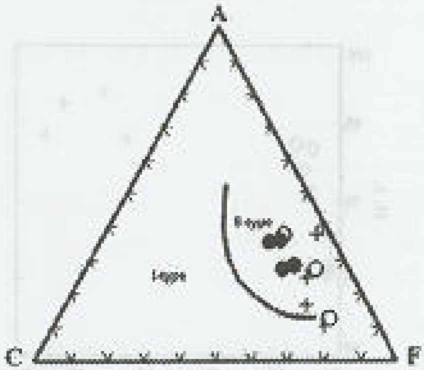

(d) Takahashi et al. (1981)

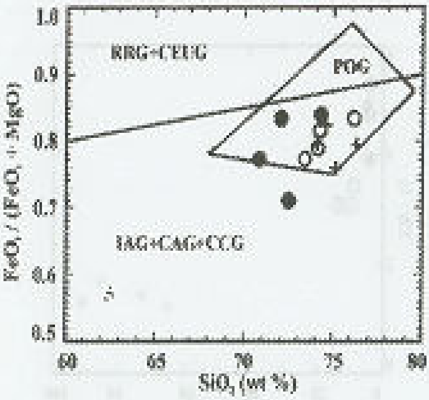

(e) Maniar and Picolli (1989)

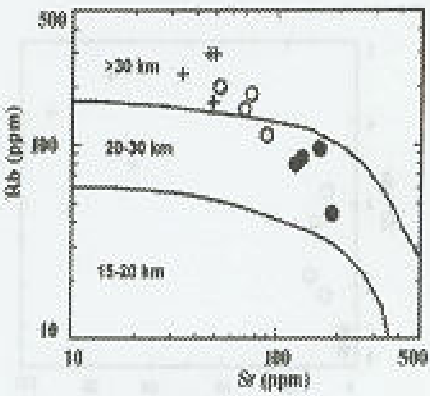

(f) Condie (1973)

Fig. 20: Classification, magma type and tectonic setting of the studied younger granites.

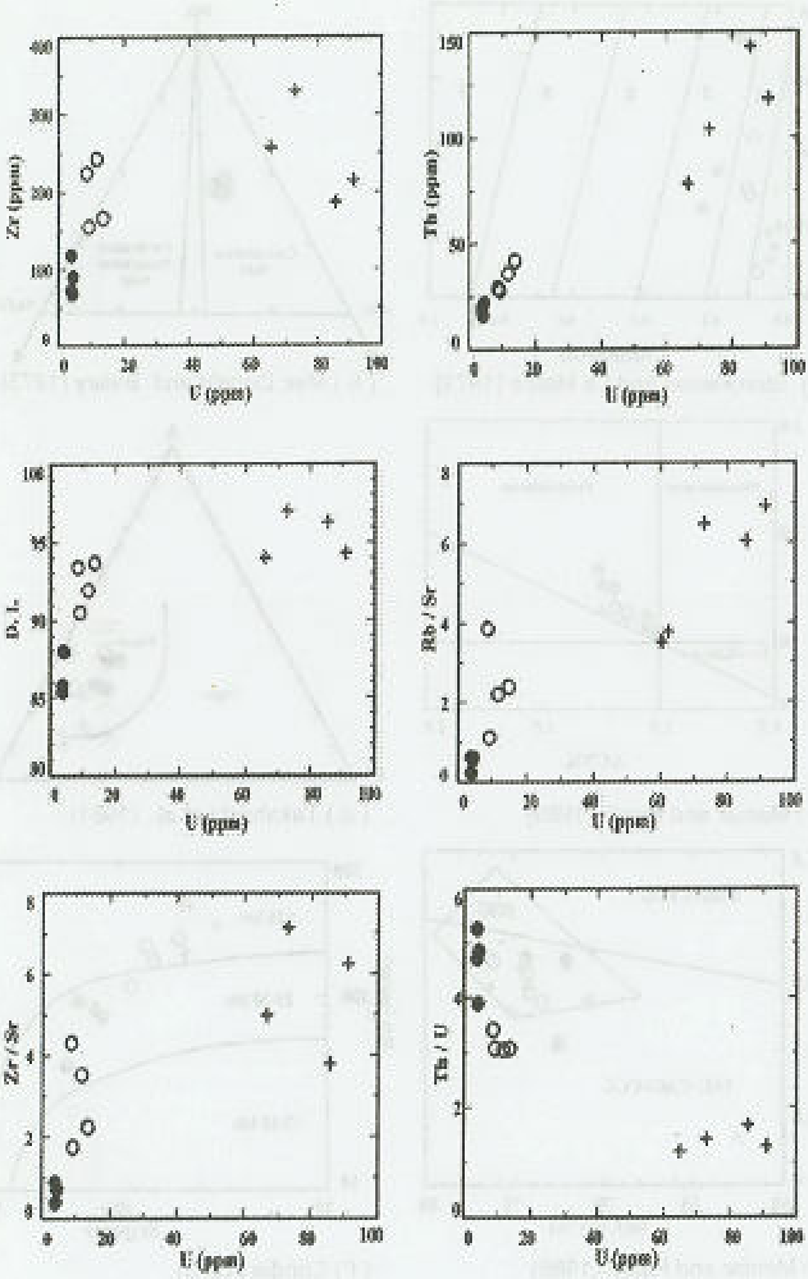

Fig. 21: U (ppm) versus some trace elements (ppm) and geochemical ratios for the studied younger granites

The studied monzogranites show Th/U ratios ranging between 4.15 and 5.53 (Fig. 21), suggesting uranium leaching, while these ratios range between 2.97 and 3.37 in syenogranites suggesting slight uranium leaching. On the other hand, the alkali-feldspar granites show ratios ranging between 1.25 and 1.68 suggesting uranium addition during post magmatic (secondary) processes.

CONCLUSIONS

The studied younger granites are classified as monzogranites, syenogranites and alkali-feldspar granites. They originated from peraluminous calc-alkaline magma. They are considered as S-type granites, derived from crustal sialic materials during post-orogenic magmatism. The crustal thickness during the emplacement of monzogranites ranges from 20 to 30 km, while both syenogranites and alkali-feldspar granites originated in a crust of thickness greater than 30 km.

The alkali-feldspar granites are considered as low Ca-granites. They possess high U-contents relative to those of monzogranites and syenogranites. The magma from which alkali-feldspar granites originated is rich in U. The enrichment of U is not only related to magmatic processes but also due to secondary processes. These secondary processes have leached uranium from the country rocks and even the monzogranites and syenogranites themselves and added it to the alkali-feldspar granites.

From the previous discussion, it is concluded that the studied younger granites are uraniferous granites enriched in both uranium and thorium. This enrichment is related to magmatic origin except minor locations, which suffered secondary processes leading to limited redistribution of uranium.

REFERENCES

Abd El-Maksoud, M.A. (1974): Geology of Abu Diab area with special emphasis on the petrogenesis of the granitic rocks. Ph.D. Thesis, Cairo Univ., Egypt.

Amin, M.S., Moustafa, G.A. and Zaatout, M.A. (1954): Geology of Abu Diab District. Geol., Mines and Quarries Dept., Cairo, Egypt, 24 p.

Assaf, H.S., Mahdy, M.A. and El Afandy, A.H., 1997, Egyptian younger granites, an approach to define parameters favouring formation of uranium deposits. 3rd Conference Geochemistry, Alexandria Univ., Egypt, pp. 409-420.

Briqueu, L., Bougault, H. and Joron, J.L., 1984, Quantification of Nb, Ta, Ti and V anomalies in magmas associated with subduction zones: Petrogenetic implications, Earth Planet. Sci. Lett., v. 68, pp. 297-308.

Condie, K.C., 1973, Archean magmatism and crustal thickening . Geol. Soc. Amer. Bull., v. 84, pp. 2981-2991.

Cox, K.G., Bell, J.D. and Pankhurst, R.J., 1979, The interpretation of igneous rocks. William Clowes, London, Britain, 414 p.

Dardier, A.M., 1997, Geology, petrology and radioactivity of some granitic masses in the area of Gabal Abu Diab, Eastern Desert, Egypt. Ph.D. Thesis, Ain Shams Univ., Egypt. 179 p.

El-Manharawy, M.S. (1977): Geochronological investigation of some basement rocks in central Eastern Desert, Egypt between lats. 25° and 26° N. Ph.D. Thesis, Cairo Univ., Egypt.

El-Mansi, M.M. (1993): Petrology, radioactivity and mineralizations of Abu- Gerida El-Erediya area, Eastern Desert, Egypt. M. Sc. Thesis, Faculty of Science, Cairo University, Cairo, Egypt, 223 p.

El-Mansi, M.M. (1996): Petrology, radioactivity and mineralization of Samut-Atud area, Central Eastern Desert, Egypt. Ph. D. Thesis, Cairo Univ., 320 p.

El-Mansi, M.M., Dardier, A.M. and Moussa, E.M (2004): Geology and Uranium Distribution within the Older Granitoids and Some Granitic Masses in the North Eastern Desert, Egypt (Egypt. Jour. Geol., in press).

Greenberg, J.K. (1981): Characteristics and origin of Egyptian younger granites. Geol. Soc. America Bull., part I, vol. 92, p. 224-256.

Hashad, A.H., Sayyah, T.A., El-Kholy, S.B. and Youssef, A. (1972): Rb/Sr isotopic age determination of some basement Egyptian granites. Egypt, Jour. Geol., vol. 16, p. 269-281.

Heier, K.S., 1973, Geochemistry of granulite facies rocks and problems of their origin. Philos. Trans. Roy. Soc., London, Series, v. 273, pp. 429-442.

Mac Donald, R., and Bailey, D. K., 1973, The chemistry of the peralkaline over saturated obsidians .U.S. Geol. Surv. Prof. Pap. 44 - No. I, 37 p.

Maniar, P.D., and Piccoli, P.M., 1989, Tectonic discrimination of granitoids. Geol. Soc. Am. Bull., No.101, pp. 635-643.

Moharem, A.F., 1999, Geology, geochemistry and radioactivity of some granitic masses in the area of Gabal El-Maghrabiya, central Eastern Desert, Egypt. Ph.D. Thesis, Faculty of Science, Ain Shams University, Cairo, Egypt, 212p.

Rogers, J.J.W. and Adams, J.S.S., 1969, Uranium. In : Wedepohl, K.H. (ed.) Handbook of geochemistry, New York, Springer-Verlag, v. 4, pp. 92 B1- 92 C10.

Sayyah, T.A., Hashad, A.H., Ibrahim, A.M. and Attawiya, M.Y. (1973): Contribution to the geochemistry of some pink granites, central Eastern Desert, Egypt. Jour. Geol., vol. 17, p.57-68.

Shapiro, L. and Brannock, W.W., 1962, Rapid analysis of silicate, carbonate and phosphate rocks.U.S. Geol. Surv. Bull. 1144A, 56 p.

Streckeisen, A. and Le Maitre, R.W., 1979, A chemical approximation to the model QAPF classification of the igneous rocks. Neus Jahrb. Mineral. Abh., v. 136, pp. 169-206.

Takahashi, M., Aramaki, S., and Ishihara, S., 1981, Magnetite-series, Ilmenite-series vs. I-type granitoids. Mining Geol. Spec. Issue, v.8, pp. 13-28.

Thronton, C.P. and Tuttle, O.F., 1960, Chemistry of igneous rocks. Differentiation Index. Am. J. Sci., v. 258, pp. 664-684.

بترولوجية وتوزيع اليورانيوم في الجرانيتات الحديثة لمنطقة جبل أبو دياب، الصحراء الشرقية، مصـــر

مدحت محمود المنسى

هيئة المواد النووية، ص.ب: ٥٣٠ – المعادى – القاهرة – مصر.

تقع منطقة جبل أبو دياب (٩٢.٥ كم٢) بين خطى عرض ١١' ٢٥° و ١٦' ٢٥° شمالاً وخطى طول ١١' ٣٤° و١٧' ٣٤° شرقاً. اعتمادا على الدراسات البتروجرافية والجيوكيميائية، أمكن تصنيف الجرانيتات الحديثة لمنطقة جبل أبو دياب إلى منزوجرانيت وسيانوجرانيت وجرانيت ذو فلسبار قلوى حيث تكونت من ماجما فوق ألومنيومية وكلس - قلوية. اشتقت هذه الماجما من مادة السيال للقشرة الأرضية أثناء النشاط الماجماتى اللاحق للحركات الأرضية. كما أوضحت الشواهد الحقلية والخصائص البتروجرافية وكذلك الخواص الجيوكيميائية أن هذه الجرانيتات الحديثة تداخلت فى صورة نبضات متلاحقة بدأت بالمنزوجرانيت وانتهت بالجرانيت ذو الفلسبار القلوى.

وترجع زيادة المحتوى اليورانيومى فى الجرانيت ذو الفلسبار القلوى إلى عمليات ماجماتية فيما عدا مناطق قليلة قد تأثرت بعمليات ثانوية أدت إلى إعادة توزيع اليورانيوم بالمنطقة حيث تم إذابته من الصخور المحيطة وكذلك من المنزوجرانيت والسيانوجرانيت وإضافته داخل الشقوق الدقيقة للجرانيت ذو الفلسبار القلوى.